

# THE MAIN THERMO-STATISTICAL MODELS OF METALLURGICAL SLAGS: THEORY AND APPLICATIONS

*J. Lehmann<sup>1)\*</sup>, In-Ho Jung<sup>2)</sup> and L. Zhang<sup>3)</sup>*

*1) ArcelorMittal Global R&D Maizières BP 30320 57 283 Maizières les, Metz Cedex, France*

*2) McGill University, Montreal, Quebec, H3A 2B2, Canada*

*3) CSIRO Process Science & Engineering, Box 312, Clayton South, Vic. 3169, Australia*

**Abstract:** Thermodynamic softwares are nowadays more and more used to understand and to control complex pyrometallurgical processes. Typically, in steelmaking shops, these tools can help the operator to better control the slag-metal reactions by optimizing slag compositions and/or stirring conditions, to define the deoxidation sequence, to better monitor the ferro-alloys additions at the different stages of the process, to minimize the refractory wear as well as refractory interactions with the melt, etc...

These computer programs, based on different procedures to minimize the Gibbs energy, contain thermodynamic models for all the involved phases and especially for slag which remains one of the most difficult to describe particularly because of the necessity to describe the Short Range Ordering phenomenon occurring in these melts over large ranges of composition. This paper gives an overview of the existing thermodynamic models of slags, especially those based on i) the quasichemical approach such as the Cell model, the Generalized Central Atom model and the Modified Quasichemical Model and ii) associated molecule or ionic species formation approach such as the Associate Model and the Reciprocal Ionic Liquid Model. The theoretical basis will be given for each model together with examples of applications to industrial pyrometallurgical processes when available.

**Keywords:** Oxide slags, thermodynamic software, quasichemical models

## 1. Introduction

Thermodynamic equilibrium computing programs are getting now a key-element of the toolbox for researchers in the steelmaking area if not yet for the engineer or operator in the steelmaking shop. It has been proven to be a valuable help for understanding and improving the process since the competition between the various reactions make it difficult to easily understand the different chemical phenomena without using these computing tools. Nowadays, a potential user has a quite large choice of commercial software FactSage [1], MPE [2], MTDATA [3] and Thermo-Calc [4] are among the most well known products. ArcelorMittal Global R&D has developed its own software CEQCSI whose ambitions are more limited than those of the commercial packages, its application domain being restricted to the steel industry whereas the others are applicable to many other industrial issues.

For the steel industry, the model used for the description of slags in these pieces of software is of utmost importance. The model must be versatile enough to deal with the diversity of the compositions met all along the production line of the steel. Ladle slags or blast furnace slags belong to what could be considered as the "basic" chemical system for metallurgical slag: the system  $\text{CaO-Al}_2\text{O}_3\text{-MgO-SiO}_2$  (CMAS), BOF or EAF slags belong to the system  $\text{CaO-FeO}_x\text{-}$

MgO-SiO<sub>2</sub>, mold slags to the system CaO-Al<sub>2</sub>O<sub>3</sub>-SiO<sub>2</sub>-Na<sub>2</sub>O-CaF<sub>2</sub>... And it is getting less and less sufficient to describe the main components of the slags since these slags are often used to purify the steel from minor or tramp elements: P<sub>2</sub>O<sub>5</sub> has typically to be added to the list of BOF slag components; with the rising production of micro-alloyed steels or of high-alloyed steels or with the constraints coming from recycling, the user would also like to have models with Ti or Cr oxides... The precision of the slag models must also be high enough for predicting with a sufficient accuracy the partition between the slag and the metal or the slag and the gas phase of the various chemical elements, some of them having to be controlled with a precision less than a few thousandths of percents or even less than a few parts per million as it is the case typically for phosphorus, sulfur, oxygen... Finally, the same models must be used for the description of liquid oxides inclusions typically in Al-killed Ca-treated steels where liquid Ca-aluminates are wished or in Si-Mn killed steels for long products where this is liquid SiO<sub>2</sub>-CaO-MnO-Al<sub>2</sub>O<sub>3</sub> which are wanted.

Therefore, during the last 20-30 years, several slag models have been built. We have chosen to present here only models included in software and which are derived from an expression of the Gibbs energy. This excludes some useful models as for instance Flood-Grothheim model [5] which is however still useful for BOF slags since it provides accurate estimations of steel P and S contents at equilibrium.

The models presented here can be classified into two categories. The first ones are based on the quasichemical approach proposed by Guggenheim [6] such as the Cell model, the Generalized Central Atom model (co-developed by ArcelorMittal Global R&D and CSIRO Process Science and Engineering and implemented in CEQCSI and in MPE [2]) and the Modified Quasichemical Model (implemented in FactSage [1]). The second category is based on the associated molecule or ionic species formation approach such as the Associate Model (implemented in MTDATA [3]) and the Reciprocal Ionic Liquid Model (implemented in ThermoCalc [4]).

## 2. Quasichemical models

The quasichemical formalism as proposed by Guggenheim [6] could be simply illustrated by the case of a binary system containing N<sub>A</sub> and N<sub>B</sub> atoms or molecules A and B with a common coordinate number z. To derive an expression of the partition function, it models the short range ordering phenomenon (SRO) by considering all possible pairs of atoms or molecules AA, AB and BB distributed on a quasilattice. The formation of AB pairs from AA and BB pairs is associated to a Gibbs energy change:



If N<sub>AA</sub>, N<sub>BB</sub> and 2N<sub>AB</sub> (we assume N<sub>AB} = N<sub>AB</sub>) denote the mole numbers of the different pairs, Guggenheim proposed to correct the expression corresponding to a random mixing of pairs:</sub>

$$g = \frac{\left(\frac{1}{2}z(N_A + N_B)\right)!}{(N_{AA})!(N_{BB})!((N_{AB})^2)} \quad (2)$$

by a multiplying factor h. Indeed, expression (Equation2) overcounts the number of configurations since it does not take into account the interaction (overlapping) between the different pairs. h is designed in such a way that for W<sub>AB}=0, the number of configurations must be equal to the number of random distributions of A and B:</sub>

$$h = \frac{(N_A + N_B)!}{N_A! N_B!} \left/ \left( \frac{\left( \frac{1}{2} z (N_A + N_B) \right)!}{(N_{AA}^*) (N_{BB}^*) ((N_{AB}^*))^2} \right) \right. \quad (3)$$

where

$$N_{ij}^* = \frac{N_i \cdot N_j}{N_A + N_B} \quad (4)$$

One of the drawbacks of the quasichemical model is that it could lead to negative configurational entropy for high deviations from randomness, i.e. very large and negative values of  $W_{AB}$  when the coordination numbers differ from 2. Hillert et al. [7] propose a correction of this drawback for binary solutions consisting in introducing an additional term function of the degree of SRO in the expression of the configurational entropy.

### 3. Cell model

The Cell model developed by ArcelorMittal Maizières (formerly IRSID) is one of the simplest models for slags derived from Guggenheim's treatment. It generalizes the approach proposed by Kapoor and Froberg [8] for ternary system. Two sublattices are supposed to exist, one filled with the cations, the other one by the anions. The structure of the slag is then described in terms of cells i-k-j consisted in a central anion k surrounding by two cations i and j. The mole number of cells i-k-j is  $R_{ij}^k$ .

One of its originalities lies in the formulation of the corrective factors h. Let us note  $(C_i)_{u_{ik}} (A_k)_{v_{ik}}$  the chemical formula of the component (i,k) and  $N_{ik}$  its mole number. All anions are assumed to have the same valency, so that we can define  $a_i$  as the ratio between cation and anion stoichiometric coefficients  $a_i = u_{ik}/v_{ik}$ . The cations are placed on their sublattice by decreasing values of their charges. Let us assume that the cations 1,2,..,i-1 are already placed on the sublattice, their "neutralize" a mole number of anionic sites such as the mole number of sites left unoccupied is equal to

$$D_i = \sum_{j=i}^m V_j \quad \text{with} \quad V_j = \sum_{k=1}^p v_{jk} N_{jk} \quad (5)$$

$V_j$  is the mole number of anionic sites "brought" by the cations j. The mole number of sites available for the cations i is

$a_i D_i$ , among them they occupy  $\sum_{k=1}^p u_{jk} N_{jk}$  and  $a_i D_{i+1} = a_i D_i - \sum_{k=1}^p u_{jk} N_{jk}$  are left unoccupied. The number of

permutations possible for the cations i is therefore:

$$P_i = \frac{(N_A a_i D_i)!}{\left( N_A \sum_{k=1}^p u_{jk} N_{jk} \right)! (N_A a_i D_{i+1})!} \quad (6)$$

And the total number of permutations for the cations  $P_C$  is computed by multiplying the  $P_i$ 's, which gives after simplification by the Stirling formula:

$$\ln P_C = N_A \sum_{i=1}^{m-1} a_i \left( D_i \ln \frac{D_i}{V_i} - D_{i+1} \ln \frac{D_{i+1}}{V_i} \right) \quad (7)$$

The corresponding term for anions is derived more easily since all the anions are supposed to have the same charge. The final expression of the degeneracy is then:

$$\ln g = N_A \left[ \sum_{i=1}^{m-1} a_i \left( D_i \ln \frac{D_i}{V_i} - D_{i+1} \ln \frac{D_{i+1}}{V_i} \right) + 2 \sum_{i=1}^m V_i \ln \frac{V_i}{D_1} - \sum_{i,j=1}^m \sum_{k=1}^p R_{ij}^k \ln \frac{R_{ij}^k}{D_1} \right] \quad (8)$$

Beside cell formation parameters  $W_{ij}^k$  associated to the formation of i-k-j cells from i-k-i and j-k-j cells, interaction energy parameters  $E_{ij}^k$  have been introduced. Both are binary parameters and function of composition such as Gibbs energy of a ternary solution is calculated from the binary parameters using the Toop-like interpolation technique with the most acidic component as an asymmetric component.

For instance, with these parameters, the Gibbs energy of a binary  $\text{SiO}_2$ -MO solution is expressed as:

$$\begin{aligned} G = & 2 \left( {}^0W_{\text{MSi}}^{\text{O}} + {}^1W_{\text{MSi}}^{\text{O}} x_{\text{SiO}_2} \right) \cdot R_{\text{MSi}}^{\text{O}} + 2R_{\text{SiSi}}^{\text{O}} \frac{N_{\text{M}}}{(2N_{\text{Si}} + M_{\text{M}})} \left( {}^0E_{\text{SiM}}^{\text{O}} + {}^1E_{\text{SiM}}^{\text{O}} x_{\text{SiO}_2} \right) \\ & + RT \left( \frac{1}{2} (2N_{\text{Si}} + M_{\text{M}}) \ln (2N_{\text{Si}} + M_{\text{M}}) - \frac{3}{2} (2N_{\text{Si}}) \ln (2N_{\text{Si}}) - \frac{3}{2} N_{\text{M}} \ln N_{\text{M}} \right) \\ & + RT \left( R_{\text{SiSi}}^{\text{O}} \ln R_{\text{SiSi}}^{\text{O}} + R_{\text{MM}}^{\text{O}} \ln R_{\text{MM}}^{\text{O}} + 2R_{\text{SiM}}^{\text{O}} \ln R_{\text{SiM}}^{\text{O}} \right) \end{aligned} \quad (9)$$

where the number of cells  $R_{ij}^k$  must be replaced by their actual values obtained by minimizing G with their respect under the mass balance constraints:

$$\begin{aligned} 2N_{\text{Si}} &= R_{\text{SiSi}}^{\text{O}} + R_{\text{SiM}}^{\text{O}} \\ N_{\text{N}} &= R_{\text{SiM}}^{\text{O}} + R_{\text{MM}}^{\text{O}} \end{aligned} \quad (10)$$

The Cell Model satisfactorily reproduces the phase diagram and the constituent activity for ternary silicate melts except for systems containing simultaneously  $\text{Al}_2\text{O}_3$  and  $\text{SiO}_2$  [9] in which only poor agreement has been reached for acid compositions close to the  $\text{Al}_2\text{O}_3$ - $\text{SiO}_2$  binary.

Despite its weaknesses, the Cell model has been proved to be a useful practical tool for steelmakers. For practical use, the model has been implemented in the CEQCSI software developed by ArcelorMittal Global R&D [10]. It covers the system  $\text{SiO}_2$ - $\text{TiO}_2$ - $\text{Ti}_2\text{O}_3$ - $\text{Cr}_2\text{O}_3$ - $\text{CrO}$ - $\text{Al}_2\text{O}_3$ - $\text{Fe}_2\text{O}_3$ - $\text{FeO}$ - $\text{MnO}$ - $\text{MgO}$ - $\text{CaO}$ - $\text{S}$ - $\text{CaF}_2$ . A former version of the Cell model is also available in ThermoCalc [4].

Figure 1 gives an example of an application of the Cell model for Al-killed Ca-treated steel. One aim of the Ca-treatment is to transform solid alumina inclusions into Ca-aluminates which one wants to be liquid at the steel casting temperature in order to avoid any clogging of the submerged entry nozzle of the continuous casting machine. With such diagrams, the steelmakers gets an idea of how much Ca is needed to successfully transform the alumina inclusions for the level of cleanliness (characterized by the total oxygen contents) usually obtained in their steel shops.

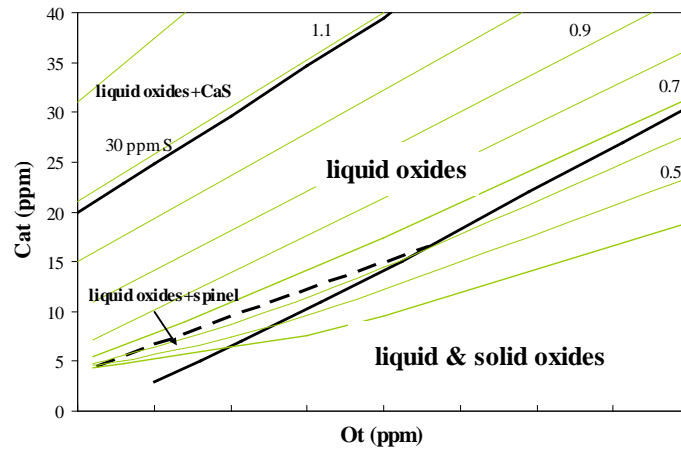


Figure 1. Domains of stability of the liquid Ca-aluminates for a given steel grade at the liquidus temperature of the grade as computed by CEQCSI. The light lines give the iso-%CaO/%Al<sub>2</sub>O<sub>3</sub> values of the Ca-aluminates.

The slag thermodynamic model, as well as all the models describing other phases, is used in another piece of software MIPPHASOLACIDO (which uses also CEQCSI solver) designed to solve transfer equations part of kinetic simulations. A test book case is presented in Figure 2 for slag/metal desulfurization. In this model, all reactions are taken into account and not only the sulfur transfer. The desulfurization process takes place through reaction with the top slag and with slag droplets. Droplets size distribution and residence time must be specified. Three situations are depicted in Figure 2: a situation where the slag is supposed to stay entirely liquid all along the reaction, a situation where the slag can partly crystallize (the amount of the different phases appearing in the slag is given in the right hand side of the figure) and a situation where this crystallization reduces the transfer coefficients proportionally to the amount of solid phases. We can see that this effect, as suggested by many plant results, cannot be neglected.

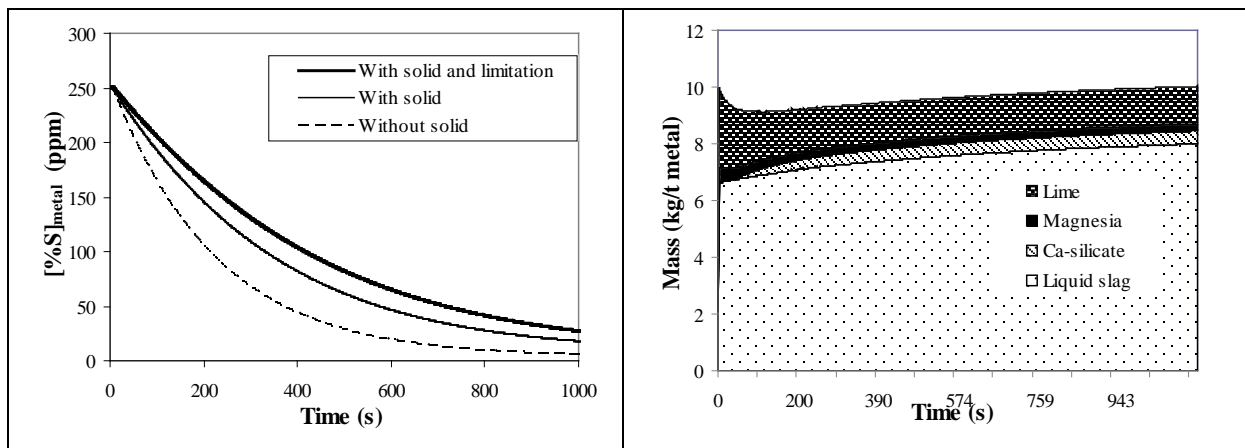


Figure 2. Slag/metal desulfurization modelling. The partial crystallization of the slag (right hand side) has a dramatic effect on the desulfurization kinetics.

In order to correct the Cell model for systems containing simultaneously Al<sub>2</sub>O<sub>3</sub> and high amounts of SiO<sub>2</sub>, Zhang et al. [11] introduced more flexible polynomial functions for the cell formation energies as well as ternary model

parameters For example, for the ternary CaO-Al<sub>2</sub>O<sub>3</sub>-SiO<sub>2</sub> system, the cell formation energy parameters  $W_{SiCa}$  and  $W_{SiAl}$  have been modified by introducing two ternary parameters  $W_{SiCaAl}$  and  $W_{SiAlCa}$  as follows:

$$W_{ij} = W_{ij}^{(0)} + W_{ij}^{(1)}x_i + W_{ij}^{(2)}x_i^2 + \sum_k W_{ijk} \frac{x_k}{(1-x_i)} \quad (11)$$

The model extended to the system SiO<sub>2</sub>-P<sub>2</sub>O<sub>5</sub>-TiO<sub>2</sub>-Ti<sub>2</sub>O<sub>3</sub>-Al<sub>2</sub>O<sub>3</sub>-Cr<sub>2</sub>O<sub>3</sub>-Fe<sub>2</sub>O<sub>3</sub>-FeO-CaO-MgO-CrO-NiO-MnO is proposed to the users through the MPE package [2].

The Cell model within the CSIRO Multi-Phase Equilibrium (MPE) software has been used for simulation of the smelting of high chromium and low Cu-Ni containing concentrates for the South African PGM (Platinum Group Metals) producers [12]. During electric smelting of these concentrates, a Cu-Ni-Fe-S matte and complex slag (SiO<sub>2</sub>-MgO-FeO<sub>x</sub>-CrO<sub>x</sub>-CaO-Al<sub>2</sub>O<sub>3</sub>-NiO-Cu<sub>2</sub>O) are produced. It is desirable to contain the Cr in the liquid slag phase and to avoid the formation of a complex spinel phase (Cr, Ni, Fe, Mg, Al)<sub>3</sub>O<sub>4</sub>, which could cause operational difficulties and result in poor metallurgical performance. Literature review and in-house measurements identified that for a given slag chemistry, temperature and oxygen potential of the slag have pronounced effects on the solubility of Cr in the slag and hence stability of the spinel phase. The validated MPE model was hence used to identify some optimum operating windows that would result in more than one order of magnitude increase in solubility of the Cr in such slags. In Figure 3, some comparisons are made between the measured [13] and calculated solubility of CrO<sub>x</sub> in the melter type slags, which are rich in SiO<sub>2</sub>, MgO and FeO<sub>x</sub> (see Table 1 for details). These Figures show how the solubility varies with oxygen potential and temperature of the slags. The excellent agreement between the experimental data and MPE results are also illustrated in this Figure.

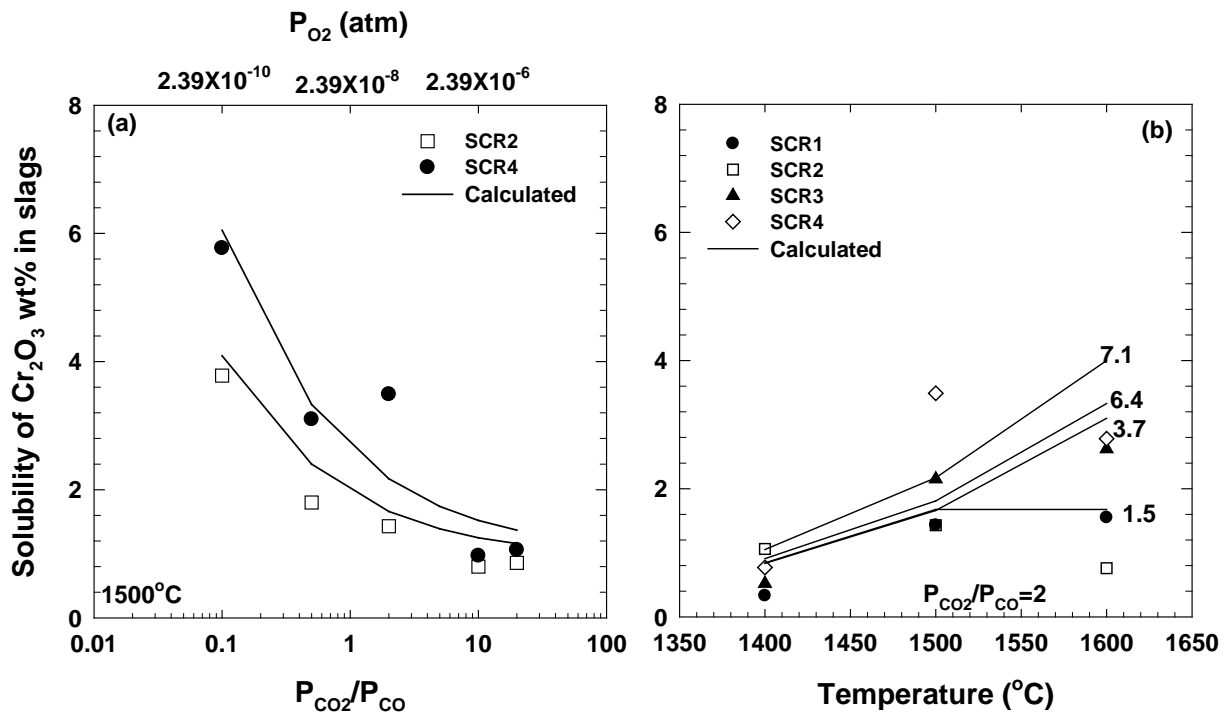


Figure 3. Comparison between the experimental data [13] and the MPE calculations on solubility of Cr as functions of (a) oxygen partial pressure in melter slags at 1500°C and (b) temperature at  $P_{CO_2}/P_{CO} = 2$ .

Table 1. The compositions used in the model calculations of the melter slag samples used for the study of Cr solubility.

Sample ID	Composition wt%					
	MgO	Cr <sub>2</sub> O <sub>3</sub>	FeO <sub>x</sub>	SiO <sub>2</sub>	CaO	Al <sub>2</sub> O <sub>3</sub>
SCR1	19	1.5	21.5	48.3	4.8	4.9
SCR2	19.8	3.7	22	44.8	4.8	4.9
SCR3	18.2	6.4	20.3	45.2	4.9	5
SCR4	14.3	7.1	18	50.5	5	5.1

#### 4. The Generalized Central Atom (GCA) model

The Generalized Central Atom (GCA) model unifies in the same formalism the Cell model and the Central Atom model originally proposed by Lupis and Elliott [14] for solid steel and very similar to the "surrounded atoms model" developed at about the same period at the LTPCM [15,16].

In the GCA model, the structure is also described in terms of cells still composed of a central atom surrounded by a shell of its nearest neighbors but also by a shell of its second-nearest neighbors. Moreover, the central atom can be either an anion or a cation. In a system with  $m$  components with  $t$  substitutional elements, a cell is noted as:

$$\begin{array}{ccc}
 i_1, i_2, \dots, i_k, \dots, i_t & \text{Second-nearest neighbors} & \\
 \mathbf{J} & \text{Central atom} & \\
 j_{t+1}, \dots, j_r, \dots, j_m & \text{Nearest neighbors} & 
 \end{array} \quad (12)$$

Similarly to the Cell model, two kinds of parameters are considered in the GCA model, namely formation and interaction energy parameter. The formation energy of the cell is noted  $\phi_{\{i\},\{j\}}^J$  where  $J$  represents the central atom and  $\{i\}$  and  $\{j\}$  presents the whole set of cations and anions present on the first- and second-nearest neighbors shells. For the sake of simplicity, the formation energy term is assumed to be the sum of the contributions of the two shells:

$$\phi_{\{i\},\{j\}}^J = \phi_{\{i\}}^J + \phi_{\{j\}}^J \quad (13)$$

To reduce the number of parameters, different assumptions can be formulated to describe the energy variation for the central atom according to the composition of the chemical neighborhood. For the formation energy, the following expression has been chosen:

$$\phi_{\{i\}}^J = \sum_{k=1}^t i_k \phi_{kk}^J + \frac{1}{2} \sum_{\substack{k,l=1 \\ k \neq l}}^t i_k i_l \phi_{kl}^J \quad (14)$$

This formula shows that the model accepts ternary parameters as for example  $\phi_{\text{SiCa}}^{\text{Al}}$ . A simple dependence on temperature and a linear dependence on composition have been introduced.

The more precise description of SRO as well as the added flexibility in the definition of the parameters solves the problem of the inaccuracy of the Cell model for silica-rich compositions of alumina bearing slags [17].

The development of the GCA model for slags is done in the framework of a cooperative work between ArcelorMittal Global R&D and CSIRO Process Science and Engineering. Presently, the model covers the system P<sub>2</sub>O<sub>5</sub>-SiO<sub>2</sub>-Al<sub>2</sub>O<sub>3</sub>-Fe<sub>2</sub>O<sub>3</sub>-FeO-MnO-MgO-CaO-Na<sub>2</sub>O-K<sub>2</sub>O-S-CaF<sub>2</sub> and its extension to Ti-oxides is underway. As an example, precision obtained for P description is illustrated in Figure 4 which compared, for a very large bunch of experimental works

collected in the literature, calculated and experimental values of P activity. Presently, the GCA model is available in the CEQCSI software for ArcelorMittal internal use and will be implemented in MPE [2].

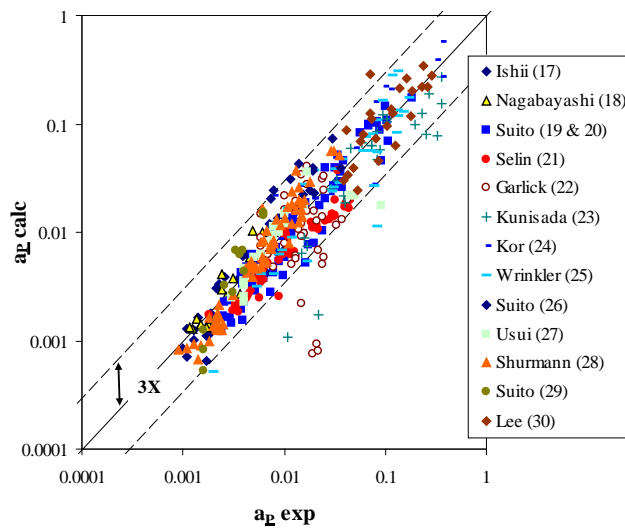


Figure 4. Comparison between P activity (ref state: 1 wt% diluted solution in liquid steel) calculated with GCA and experimental [18- 31].

The model has been used to compare P equilibrium values to actual P contents resulting from slag/metal reactions in two different Blast Oxygen Furnaces of ArcelorMittal (Figure 5). These two furnaces are equipped differently. In the first one (Plant A), blowing is operated mostly through bottom tuyeres (the ratio between bottom and top blowing is around 70-30%) whereas in the second one (Plant B) the ratio between bottom and top blowing is only 30-70%. Therefore, it is not surprising that P equilibrium is reached in Plant A and not in Plant B.

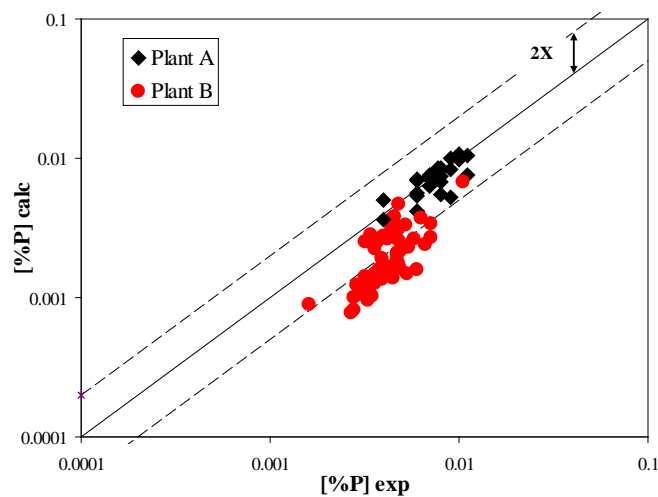


Figure 5. Comparison between calculated equilibrium phosphorus contents and actual values for two different ArcelorMittal BOF's.



## 5. The Modified Quasichemical Model

The Modified Quasichemical Model (MQM) was first introduced by Pelton and Blander [32,33]. The most recent version of the model is discussed in a series of articles [34-37]. The short range ordering in molten silicates is taken into account in a similar way as in the Cell model by considering quasichemical reactions as the following one:



The molar Gibbs energy of the reactions, as  $\Delta g_{MSi}$ , are the main parameters of the model and are written as polynomials function of composition and temperature. The molar Gibbs energy of a binary solution MO-SiO<sub>2</sub> is expressed as:

$$G^m = \left( x_{MO} g_{MO}^0 + x_{SiO_2} g_{SiO_2}^0 \right) + \left( Z_M x_{MO} + Z_{Si} x_{SiO_2} \right) x_{MSi} \Delta g_{MSi} / 4 + \\ RT \left( x_{MO} \ln x_{MO} + x_{SiO_2} \ln x_{SiO_2} \right) + \\ RT \frac{Z_M x_{MO} + Z_{Si} x_{SiO_2}}{2} \left( x_{MM} \ln \frac{x_{MM}}{Y_{MO}^2} + x_{SiSi} \ln \frac{x_{SiSi}}{Y_{SiO_2}^2} + x_{MSi} \ln \frac{x_{MSi}}{2Y_{MO} Y_{SiO_2}} \right) \quad (16)$$

where  $x_{MM}$ ,  $x_{SiSi}$  and  $x_{MSi}$  are the pair fractions,  $Z_M$  and  $Z_{Si}$  are the second-nearest-neighbor coordination numbers of M and Si ( $Z_{Si}/Z_M$  is the valency ratio of Si and M cations), and  $Y_{MO}$  and  $Y_{SiO_2}$  are weighted mole fractions defined as:

$$Y_{SiO_2} = \left( 1 - Y_{MO} \right) = Z_{Si} x_{SiO_2} / \left( Z_M x_{MO} + Z_{Si} x_{SiO_2} \right) \quad (17)$$

The values of pair fractions at equilibrium are determined by setting  $\partial G^m / \partial x_{MSi} = 0$  under mass balance constraints.

Contrary to the Cell model or to the GCA model, the values of the coordination numbers are among the parameters that could be fitted on experimental data and thus they could differ from the real ones.

For ternary systems, different extrapolation techniques of the binary parameters can be applied depending on the nature of the components. This flexibility gives to the MQM a high ability to model multicomponent systems. For instance, in the case of the CaO-Al<sub>2</sub>O<sub>3</sub>-SiO<sub>2</sub> aluminosilicate system, either the Kohler-type or the Toop-type interpolation technique can be used and, actually, the MQM uses the Toop-type interpolation technique for ternary aluminosilicate melts with SiO<sub>2</sub> as an asymmetric component [38].

As the Cell model or the GCA model, the MQM model has been applied to many industrial applications and especially to steelmaking operations for slag/metal reactions, inclusion control and reactions with refractory. To this purpose, it has been included in the commercially available FactSage software [1], introduced in 2001 as the fusion of the F\*A\*C\*T/FACT-Win (Thermfact, Canada) and ChemSage (GTT-Technology, Germany) thermochemical packages. The FactSage oxide solution database (FToxid) contains consistently assessed and critically evaluated thermodynamic data for the molten slag phase, numerous extensive ceramic solid solution phases and all available stoichiometric compounds containing SiO<sub>2</sub>-CaO-MgO-Al<sub>2</sub>O<sub>3</sub>-FeO-Fe<sub>2</sub>O<sub>3</sub>-MnO-TiO<sub>2</sub>-Ti<sub>2</sub>O<sub>3</sub>-CrO-Cr<sub>2</sub>O<sub>3</sub>-ZrO<sub>2</sub>-NiO-CoO-Na<sub>2</sub>O-K<sub>2</sub>O-B<sub>2</sub>O<sub>3</sub>-Cu<sub>2</sub>O-As<sub>2</sub>O<sub>3</sub>-GeO<sub>2</sub>-PbO-SnO-ZnO. The core Al<sub>2</sub>O<sub>3</sub>-CaO-FeO-Fe<sub>2</sub>O<sub>3</sub>-MgO-SiO<sub>2</sub> system has been fully optimized from 25 °C to above the liquidus temperatures at all compositions and oxygen partial pressures. Components like B<sub>2</sub>O<sub>3</sub>, K<sub>2</sub>O, Na<sub>2</sub>O, CoO, CrO, Cr<sub>2</sub>O<sub>3</sub>, Cu<sub>2</sub>O, MnO, NiO, PbO, SnO, TiO<sub>2</sub>, Ti<sub>2</sub>O<sub>3</sub>, ZnO and ZrO<sub>2</sub> were added to

this core six-component system and the relevant subsystems were optimized over the composition ranges important for industrial applications. The dilute solubilities of gaseous species such as F, S, SO<sub>4</sub>, PO<sub>4</sub>, H<sub>2</sub>O, OH, C, CO<sub>3</sub>, CN, Cl, and I are also modeled using the Blander-Reddy hybrid Capacity Model [39-42].

Recently, the two-sublattice MQM [36,37] has been developed with quadruplet approximation in which the basic entity to define the configurational entropy contains two cations and two anions. The parameters of the original model which have been previously optimized for oxide melts can be easily included in the two sublattice MQM without losing any accuracy. The two-sublattice model has been successfully applied to molten slag containing sulfur [43] and fluorine [44]. The expansion of oxide slag toward sulfide can be helpful to understand the for example the evolution of oxisulfide inclusion during secondary steelmaking and even downstream process. The purpose of the recent expansion of the slag database to fluoride system is to perform various thermodynamic calculations for fluoride containing slags including impurity control in steel, refractory corrosion and mould flux solidification.

The example in Figure 6 concerns Si-Mn killed steel for tire-cord. It shows the change of composition of initially Mn-alumino-silicates inclusions by reaction with an appropriate composition of slag rich in CaO. The benefit of such treatment is to further decrease the melting point of these inclusions [45] by incorporation in their chemistry of some amounts of CaO.

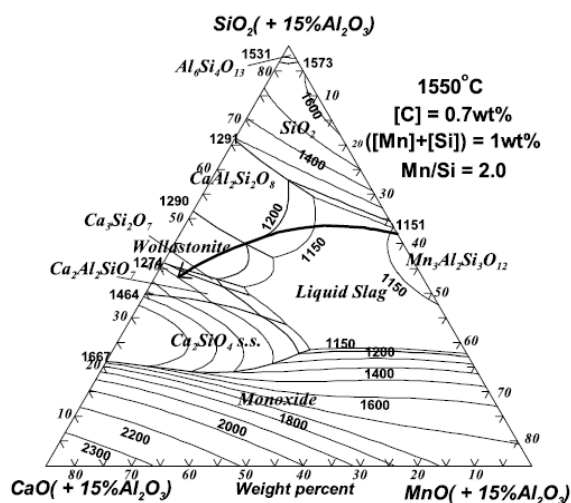


Figure 6. Calculated change of composition of inclusions formed during Mn/Si deoxidation (as shown by arrows) by reaction with CaO-containing top slag at 1550°C (top slag composition: 55wt% CaO–15wt% Al<sub>2</sub>O<sub>3</sub>–30wt% SiO<sub>2</sub>). Predicted liquidus isotherms (in °C) are also plotted.

Figure 7 shows the calculated liquidus projection for the CaO-SiO<sub>2</sub>-CaF<sub>2</sub> system which is one of the most important oxy-fluoride systems for metallurgical applications. Thermodynamic properties of cuspidine (Ca<sub>4</sub>Si<sub>2</sub>F<sub>2</sub>O<sub>7</sub>) and its primary solidification range are well reproduced.

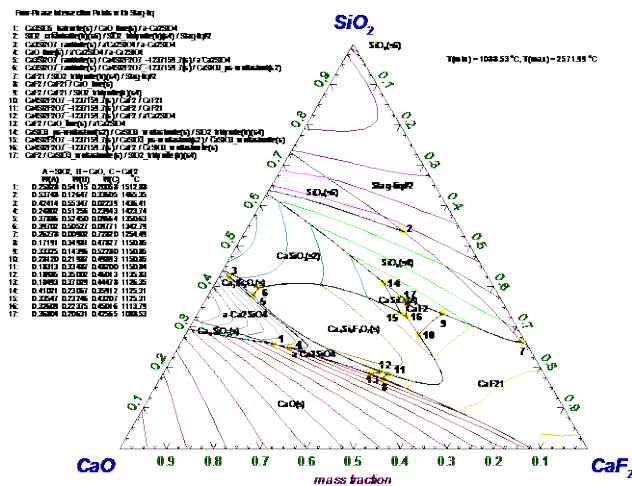


Figure 7. Calculated liquid projection of the CaO-SiO<sub>2</sub>-CaF<sub>2</sub> system.

It is well-known that CaF<sub>2</sub> containing slag is very corrosive for refractory lining such as MgO-C refractory. Phase diagram information is very essential to design the optimum slag composition to minimize such corrosion process. However, the experimental multicomponent phase diagrams for CaF<sub>2</sub> containing oxide system are unavailable in many cases for steelmaking applications and therefore the calculated phase diagrams from thermodynamic modeling are very valuable. Figure 8 shows the influences of CaF<sub>2</sub> and Al<sub>2</sub>O<sub>3</sub> on the MgO and Ca<sub>2</sub>SiO<sub>4</sub> saturations in the CaO-MgO-SiO<sub>2</sub> system at 1600 °C.

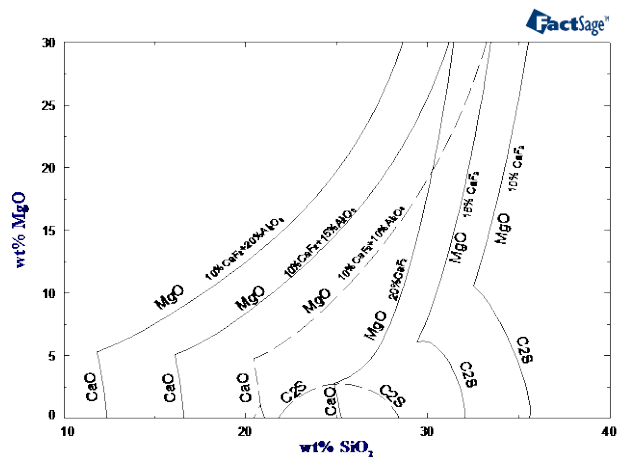


Figure 8. Calculated phase diagram and liquidus for the CaO-SiO<sub>2</sub>-MgO-Al<sub>2</sub>O<sub>3</sub>-CaF<sub>2</sub> system at 1600 °C. Influences of CaF<sub>2</sub> and Al<sub>2</sub>O<sub>3</sub> on the liquidus of the CaO-MgO-SiO<sub>2</sub> system.

Mold flux can contain a significant amount of Na<sub>2</sub>O and CaF<sub>2</sub>. Thus, the solidification temperature of mold flux can decrease even below 1100 °C. As well-known, the solidification behavior of the mould flux is one of the key factors of controlling the heat flux of steel solidification. In spite of its importance, there are no systematic study of the solidification of mould flux, because the difficulty in experiment of the slag system containing Na<sub>2</sub>O and CaF<sub>2</sub>. Thus, most of the industrial mold flux was still developed by the trial and error approach. The thermodynamic modeling can be a powerful tool for this application.

For example, the solidification of a commercial mould flux is calculated in Figure 9. The cuspidine ( $\text{Ca}_4\text{Si}_2\text{F}_2\text{O}_7$ ) phase is formed as a primary phase during the solidification at about  $1200^\circ\text{C}$ , which is consistent with experimental data. The solidifications of various mould fluxes with different starting temperature of cuspidine phase were calculated using the recent database and the results are in good agreement with experimental data. This kind of calculation can be used for the industrial mould flux development, which can significantly save time and cost.

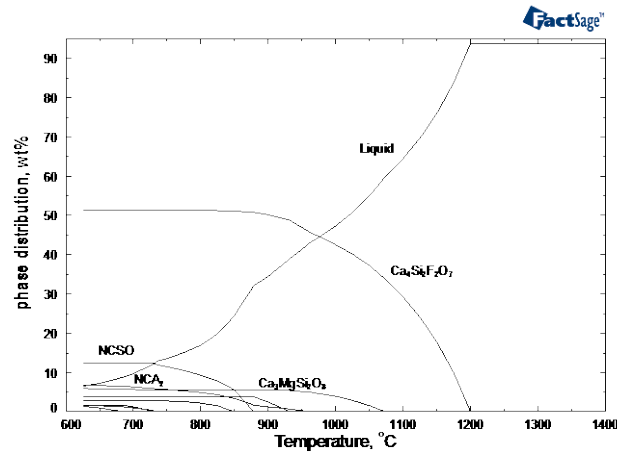


Figure 9. Scheil solidification calculation for mould flux: 31.8 $\text{SiO}_2$ -32.5 $\text{CaO}$ -0.9 $\text{MgO}$ -5.3 $\text{Al}_2\text{O}_3$ -9.5 $\text{Na}_2\text{O}$ -12.9 $\text{CaF}_2$ -0.7 $\text{Li}_2\text{O}$  in wt %.

One of the ultimate goals of the thermodynamic database is the application to industrial process simulation. Recently a new approach to model the complex industrial RH process using thermodynamic database and simplified kinetic expressions to account for the process dynamics has been developed [46]. The RH degassing vessel is an important metallurgical reactor involving complex reactions between molten steel, gas, slag, inclusions and refractory. The evolution of the metal and slag composition during the RH treatment was treated using an *effective equilibrium reaction zone model*. In this approach, all phases within the ‘effective’ reaction zone located at a reaction interface are assumed to reach equilibrium. This approach allows easy linkage of the thermodynamic database to the kinetic simulation. Depending on the process conditions, the extent of the effective reaction zone volume changes to consider the variations in reaction kinetics. The RH degassing process was divided into 14 effective reaction zones, as depicted in Figure 10. In the RH vessel, seven effective reaction zones can be identified to deal with the decarburization, deoxidation, alloying and slag/steel/refractory reactions. The steel in the ladle was divided into two effective reaction zones to take into account strong mixing in the re-circulating zone and the presence of a dead zone, where steel with lower velocity mixes more slowly. Also, effective reaction zone volumes are added to consider the reactions between steel, slag and refractory. Through FactSage macro-processing routine, the input process condition and output of the chemistry and temperature of steel, slag, refractories and gas can be read from and written to Microsoft-Excel program.

The evolution of the effective reaction zone volumes as a function of the RH process conditions were determined based on physical descriptions of the different reaction mechanisms. The evolutions of steel composition in ladle and slag composition in RH bottom vessel are calculated in Figure 11. The calculated carbon and oxygen content of ladle steel are in excellent agreement with plant sampling data in 270 ton ladle. Only a few model parameters (size of reaction zone) were introduced to reproduce the evolution of the O and C contents in the steel based on industrial

sampling data. The model is able to successfully reproduce the industrial data for various steel compositions and process conditions.

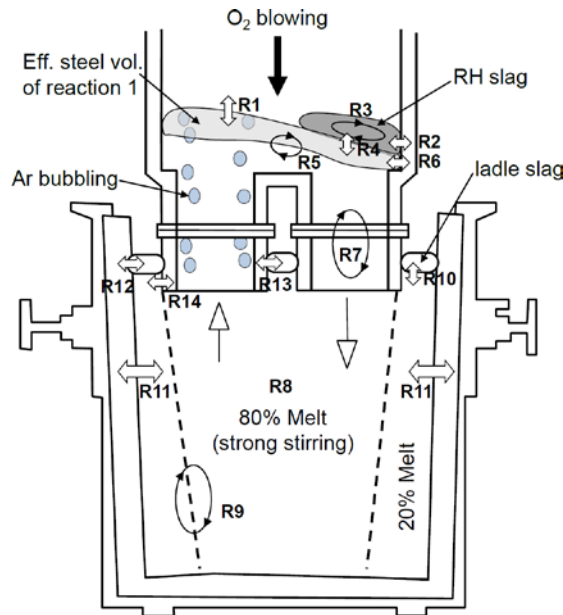


Figure 10: Schematic representation of the reaction zones in the RH degassing process.

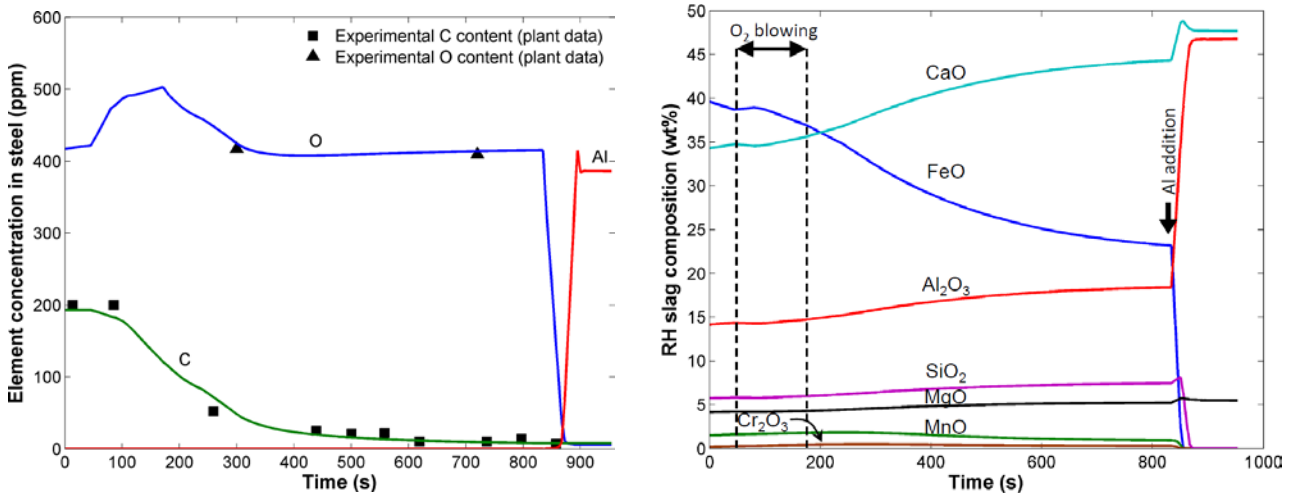


Figure 7: Evolutions of the steel composition in ladle and slag composition in RH bottom vessel during the RH degassing treatment of low-carbon steel.

The evolution of slag in RH bottom vessel is important factor for RH refractory wear. The slag composition is changing largely from CaO-FeO-Al<sub>2</sub>O<sub>3</sub>-SiO<sub>2</sub> slag in the early stage of the process to CaO-Al<sub>2</sub>O<sub>3</sub>-MgO slag in the late stage of the process after Al deoxidation. The two representative RH slag compositions in Figure 11 have been used for the RH refractories wear experiments [47,48]. The experimental results were compared with plant post-mortem refractories and gave more deep understanding of the RH refractories wear mechanism.

## 6. Associate Model

The associate model considers the existence of "associates" or molecules in the liquid whose composition could be chosen arbitrarily. For instance, the binary CaO-SiO<sub>2</sub> has been modeled by considering as associates Ca<sub>2</sub>SiO<sub>4</sub> and CaSiO<sub>3</sub> in addition to the end-member species, CaO and SiO<sub>2</sub> [49]. If we consider the simple case of a binary MO-SiO<sub>2</sub> with different associates M<sub>x</sub>SiO<sub>2+x</sub>, the molar Gibbs energy is written as a function of the fractions of species (i.e. end-members and associates) assuming a random distribution of the species and including an excess term expressed as a Redlich-Kister polynomial:

$$G^m = \sum_{i=\text{species}} x_i g_i^0 + RT \sum_{i=\text{species}} x_i \ln x_i + \sum_{i,j=\text{species}} x_i x_j \sum_{k \geq 0}^k L_{ij} (x_i - x_j)^k \quad (18)$$

The main parameters of the associate model are the energies associated to the formation of the associates as for instance:



Contrary to the quasi-chemical models, the associate model does not include any correction term in its expression of the configurational entropy. It can be easily seen that the entropy does not reduce to the ideal random mixing model when the parameters as  $\Delta g_{x\text{M}-\text{Si}}^0$  are equal to 0. This has been termed the "entropy paradox" [50].

Despite this drawback and despite the fact that the Associate Model may introduce a wrong configurational entropy in dilute solutions [34], the thermodynamic properties of binary oxide melts can be easily reproduced. The ternary and multicomponent systems can be relatively well managed with additional associates and interaction parameters. Recently, Besmann et al. [51,52] and Yazhenskikh et al. [53,54] have built up databases for the CaO-Na<sub>2</sub>O-Al<sub>2</sub>O<sub>3</sub>-B<sub>2</sub>O<sub>3</sub>-SiO<sub>2</sub> and Na<sub>2</sub>O-K<sub>2</sub>O-Al<sub>2</sub>O<sub>3</sub>-SiO<sub>2</sub> systems, respectively.

The associate model is implemented in several commercial software as, for instance, MTDATA [55] developed by the National Physical Laboratory (NPL), UK.

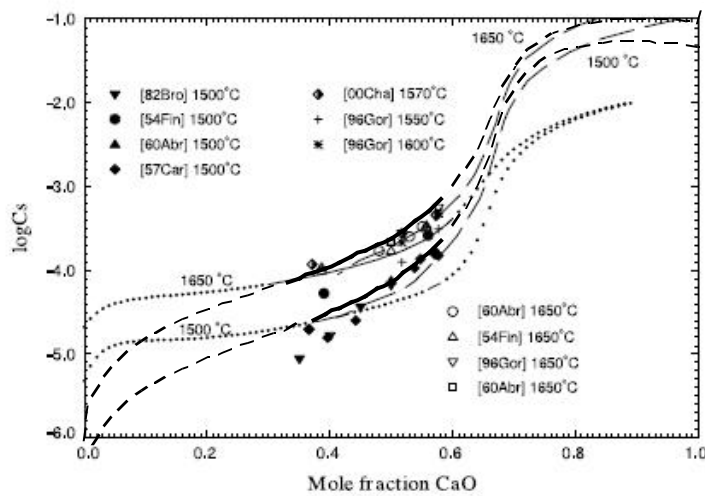


Figure 8. Comparison with experimental data [56- 62] of the predictions of sulphide capacities by MQM (FactSage, solid and dotted lines), associate model (MTDATA dashed lines) and GCA model (CEQCSI, heavy and dotted lines).

As an example of practical applications, the prediction of the sulfide capacities is an important output for all models of metallurgical slags. Figure 9 compares the predictions on the binary CaO-SiO<sub>2</sub> of the associate model (MTDATA), the MQM (FactSage) and GCA model (CEQCSI). All three models manage quite well to reproduce the experimental data even if the extrapolations to liquid metastable domains differ.

## 7. The Reciprocal Ionic Liquid Model

The Reciprocal Ionic Liquid Model (RILM) was developed by Hillert et al. [63] and is implemented in ThermoCalc [4]. This model supposes two sublattices in liquid oxides, but, contrary to the models presented before, it does not include any description of SRO. As an example, the liquid structure of the CaO-MgO-SiO<sub>2</sub> system [64] is formulated as:



where P and Q indicate the numbers of sites on each sublattice which vary with composition in order to maintain electron neutrality:

$$\begin{aligned} P &= 4y_{\text{SiO}_4^{4-}} + 2y_{\text{O}^{2-}} \\ Q &= 2y_{\text{Ca}^{2+}} + 2y_{\text{Mg}^{2+}} \end{aligned} \quad (21)$$

$Y_i$  is the site fraction of a species "i" on a particular sublattice.

The molar Gibbs energy of the ternary CaO-MgO-SiO<sub>2</sub> solution is given by:

$$\begin{aligned} G^m &= y_{\text{Ca}^{2+}} y_{\text{SiO}_4^{4-}} G_{(\text{Ca}^{2+})_4(\text{SiO}_4^{4-})_2} + y_{\text{Mg}^{2+}} y_{\text{SiO}_4^{4-}} G_{(\text{Mg}^{2+})_4(\text{SiO}_4^{4-})_2} + \\ & y_{\text{Ca}^{2+}} y_{\text{O}^{2-}} G_{(\text{Ca}^{2+})_2(\text{O}^{2-})_2} + y_{\text{Mg}^{2+}} y_{\text{O}^{2-}} G_{(\text{Mg}^{2+})_2(\text{O}^{2-})_2} + \\ & Q y_{\text{SiO}_2^0} G_{\text{SiO}_2^0} + \text{PRT} \left( y_{\text{Ca}^{2+}} \ln y_{\text{Ca}^{2+}} + y_{\text{Mg}^{2+}} \ln y_{\text{Mg}^{2+}} \right) + \\ & \text{QRT} \left( y_{\text{SiO}_4^{4-}} \ln y_{\text{SiO}_4^{4-}} + y_{\text{O}^{2-}} \ln y_{\text{O}^{2-}} + y_{\text{SiO}_2^0} \ln y_{\text{SiO}_2^0} \right) + G^E \end{aligned} \quad (22)$$

The G's parameters are the molar Gibbs energy of liquids corresponding to the subscripted formulae. In particular,  $G_{(\text{Ca}^{2+})_4(\text{SiO}_4^{4-})_2}$  and  $G_{(\text{Mg}^{2+})_4(\text{SiO}_4^{4-})_2}$  correspond to liquids of respective formulae Ca<sub>2</sub>Si<sub>2</sub>O<sub>8</sub> and Mg<sub>2</sub>Si<sub>2</sub>O<sub>8</sub> and they are the main parameters of the model.  $G^E$  is the excess Gibbs energy expanded as the Redlich-Kister polynomial of the site fractions. The thermodynamic description of the RILM for the binary MO-SiO<sub>2</sub> solution is identical to that of the associate model considering only M<sub>2</sub>SiO<sub>4</sub> associate species.

Many binary and ternary systems have been described with the RILM as CaO-Al<sub>2</sub>O<sub>3</sub>-SiO<sub>2</sub> [65], MgO-Al<sub>2</sub>O<sub>3</sub>-SiO<sub>2</sub> [66], Ca-Fe-O-Si [67] or CaO-MgO-Al<sub>2</sub>O<sub>3</sub> [68].

## 8. Conclusion

During the last decades, thermodynamic models included in powerful software have made enormous progress. The description they provide for multicomponent systems is getting more and more precise, allowing "safer and safer" applications to industrial problems. However, they all individually present some limitations: possible prediction of negative configurational entropy for quasichemical models, entropy paradox for associate models, lack of SRO description for RILM. Some ideas have been proposed to solve some of these problems as the additional entropy term for the quasichemical models [7] and they should be further explored even if they will finally require intensive re-assessment work.

Due to the success of these models, users ask more and more for applications outside the domains where the models have been assessed and where experimental data are sufficient quantitatively and qualitatively. This can be linked to the use of new primary iron sources containing traces of elements which can be potentially detrimental to the quality of the final products (e.g. Nb or V-bearing iron ores). This can also be linked to the elaboration of new high alloyed grades for which the traditional slag compositions are not satisfying (e.g. TRIP and TWIP steels vs. mold slags) or to the use of refractory products containing "unusual" oxides (e.g. Zr oxides). This shows clearly the need of new experimental works, which means certainly the need to build up new competencies since, due to the lack of funding for such works during the last 20 years, quite a lot of teams specialized in experimental studies on oxide systems have disappeared.

Thermodynamic models are also part of kinetic models which are also more and more demanded since most of the industrial processes do not reach the equilibrium state and, if they do, it is of obvious economical interest to know how long it takes for them to reach it and which actuators can be used to accelerate the process. Other quantities than phase diagrams and activities are also necessary for these kinetic models. If some quantities are starting to be well documented and modeled as slag viscosities, other are poorly known as surface energy for which a breakthrough in the experimental techniques is certainly needed.

## References

- [1] C.W. Bale, E. Bélisle, P. Chartrand, S.A. Deckerov, G. Eriksson, K. Hack, I.-H. Jung, Y.-B. Kang, J. Melançon, A.D. Pelton, C. Robelin, S. Petersen, FactSage thermochemical software and databases-recent developments, *Calphad* 33 (2009) 295-311.
- [2] L. Zhang, S. Jahanshahi, S. Sun, C. Chen, B. Bourke, S. Wright, M. Somerville, CSIRO's multiphase reaction models and their industrial applications, *JOM* 54 (2002) 51-56.
- [3] MTDATA: Teddington, UK, [www.npl.co.uk](http://www.npl.co.uk).
- [4] J.-O. Andersson, T. Helander, L. Höglund, P. Shi, B. Sundman, Thermo-Calc & DICTRA, computational tools for materials science, *Calphad* 26 (2002) 273-312..
- [5] H. Flood, K. Grojtheim, *J. Iron and Steel Inst.* 171 ( 1952) 64
- [6] E. A. Guggenheim: *Mixtures*, 1952, Oxford, Clarendon Press
- [7] M. Hillert, M. Selleby, B. Sundman, An attempt to correct the quasichemical model, *Acta Materialia* 57 (2009) 5237-5244.



- [8] M.L. Kapoor, M.G. Froberg, Theoretical treatment of activities in silicate melts, Chemical Metallurgy of Iron and Steel, Iron and Steel Institute, London, 1973, pp. 17-22.
- [9] H. Gaye, J. Welfringer, Modelling of the thermodynamic properties of complex metallurgical slags, Proc. AIME Symposium on Metallurgical Slags and Fluxes, TMS-AIME, Warrendale, PA (1984) 357-379.
- [10] J. Lehmann, Application of ArcelorMittal Maizières thermodynamic models to liquid steel elaboration, Rev. Metall. 105 (2008) 539-550
- [11] L. Zhang, S. Sun, S. Jahanshahi, An approach to modeling  $Al_2O_3$  containing slags with cell model, J. Phase Equilib. Diff. 28 (2007) 121-129.
- [12] L. Zhang, S. Sun and S. Jahanshahi, "Modelling Cr Containing Slags for PGM Smelting", MOLTEN2009, Eds., M. Sanchez, R. Parra, G. Riveros and C. Diaz, Proceedings of the VIII International Conference on Molten Slags, Fluxes and Salts, 18-21 January 2009, Santiago, Chile CD-ROM, p 391-401.
- [13] N.J. Bartie, "The effect of temperature, slag chemistry and oxygen partial pressure on the behaviour of Chromium oxide in melter slags", Master thesis of University of Stellenbosch, South Africa, 2004.
- [14] C.H.P. Lupis, J.F. Elliott, Prediction of enthalpy and entropy interaction coefficients by the « central atoms » theory, *Acta Met.*, 15 (1967) 265-276.
- [15] J.C. Mathieu, F. Durand, E. Bonnier, "L'atome entouré, entité de base d'un modèle quasi-chimique de solution binaire, I. Traitement général", *J. Chim. Phys.*, 62 (1965) 1289-1296.
- [16] B. Pascal, J.C. Mathieu, P. Hicter, P. Desré, E. Bonnier, "L'atome entouré, entité de base d'un modèle quasi-chimique de solution binaire, VII. Traitement général d'une solution interstitielle", *J. Chim. Phys.*, 68 (1971) 774-781.
- [17] L. Zhang, J. Lehmann, Application of the generalized central atom model to oxide slags, Molten 2009, Santiago, Chile (2009) 403-411.
- [18] H. Ishii and R.J. Fruhan: Iron Steelmaker, 24 (1984) 47-54.
- [19] R. Nagabayashi, M. Hino and S. Ban-ya, *Tetsu-to-Hagane*, 74 (1988) 1577-1584.
- [20] H. Suito, R. Inoue and M. Takeda: Trans ISIJ, 21 (1981) 250-259.
- [21] H. Suito and R. Inoue, Trans ISIJ, 22 (1982) 869-877.
- [22] R. Selin: *Scandinavian Journal of Metallurgy*, 20 (1991) 279-299.
- [23] S. Jahanshahi and G.R. Belton: Fifth Int. Iron and Steel Congress: Process Technology Proc. Vol.6, Washington DC, (1986), ISS, pp.641-651.
- [24] K. Kunisada and H. Iwai, Trans ISIJ, vol. 27 (1987), pp. 332-339.
- [25] G.J.W. Kor: Met. Trans., 8B (1977) 107-113.
- [26] T.B. Winkler and J. Chipman: Trans. AIME., 167 (1946) 111-133.
- [27] H. Suito and R. Inoue, Trans ISIJ, 35 (1995) 266-271.
- [28] T. Usui, K. Yamada, Y. Kawal, S. Inoue, H. Hiroaki and Y. Nimura, *Tetsu-to-Hagane*, 77 (1991) 1641-1648.
- [29] E. Schurmann and H. Fischer: Steel Research, 62 (1991) 303-313.
- [30] H. Suito and R. Inoue, Trans ISIJ, 24 (1984) 47-53.
- [31] C.M. Lee and R.J. Fruhan: Ironmaking and Steelmaking, 32(2005) 503-508.
- [32] A.D. Pelton, M. Blander, Computer-assisted analysis of the thermodynamic properties and phase diagrams of slags, in: Proc. AIME Symposium on Metallurgical Slags and Fluxes, TMS-AIME, Warrendale, PA (1984) 281-294.

- [33] A.D. Pelton, M. Blander, Thermodynamic analysis of ordered liquid solutions by a modified quasichemical approach - application to silicate slags, *Metall. Trans. B* 17B (1986) 805-815.
- [34] A.D. Pelton, S.A. Decterov, G. Eriksson, C. Robelin, Y. Dessureault, The modified quasichemical model \_ I binary solutions, *Metall. Mater. Trans. B* 31B (2000) 651-660.
- [35] A.D. Pelton, P. Chartrand, The modified quasichemical model II – multicomponent solutions, *Metall. Mater. Trans. A* 32A (2001) 1355-1360.
- [36] P. Chartrand, A.D. Pelton, The modified quasichemical model III – two sublattices, *Metall. Mater. Trans. A* 32A (2001) 1397-1408.
- [37] A.D. Pelton, P. Chartrand, The modified quasichemical model IV – two sublattice quadruplet approximation, *Metall. Mater. Trans. A* 32A (2001) 1409-1416.
- [38] G. Eriksson, A.D. Pelton, Critical evaluation and optimization of the thermodynamic properties and phase diagrams of the CaO-Al<sub>2</sub>O<sub>3</sub>, Al<sub>2</sub>O<sub>3</sub>-SiO<sub>2</sub> and CaO-Al<sub>2</sub>O<sub>3</sub>-SiO<sub>2</sub> systems, *Metall. Trans. B* 24B (1993) 807-816.
- [39] A.D. Pelton, G. Eriksson, JA Romero-Serrano, Calculation of sulfide capacities of multicomponent slags, *Metall. Trans. B* 24B (1993) 817-825.
- [40] A.D. Pelton, Thermodynamic calculation of gas solubilities in oxide melts and glasses, *Glastechnische Berichte* 72 (1999) 214-226.
- [41] I.-H. Jung, Thermodynamic modeling of gas solubility in molten slags (I) – carbon and nitrogen, *ISIJ Inter.* 46 (2006) 1577-1586.
- [42] I.-H. Jung, Thermodynamic modeling of gas solubility in molten slags (II) – water, *ISIJ Inter.* 46 (2006) 1587-1593.
- [43] Y.-B. Kang, A.D. Pelton, Thermodynamic model and database for sulfides dissolved in molten oxide slags, *Metall. Mater. Trans. B* 40B (2009) 979-994.
- [44] I.-H. Jung, Thermodynamic modeling of the CaF<sub>2</sub> containing slags and its applications to steelmaking processes, in: *Asia Steel Conf. 2009*, Pusan Korea, paper S3-30.
- [45] I.-H. Jung, S. Decterov, A.D. Pelton, Y.-B. Kang, H.-G. Lee, Critical thermodynamic evaluation and optimization of the CaO-MnO-Al<sub>2</sub>O<sub>3</sub>-SiO<sub>2</sub> system and application to inclusion control, in: K.S. Coley, G. Brooks (Eds.), *Proc. CIM Symposium, Ladle and Tundish Technology*, Canadian Institute of Metallurgy, Montreal, 2002, 131-147.
- [46] M.-A. Van Ende, Y.-M. Kim, M.-K. Cho, J. Choi, I.-H. Jung, A Kinetic model for the Ruhrstahl Heraeus (RH) Degassing process, *Metall. Mater. Trans. B*, 2011, 477-489.
- [47] M.-A. Van Ende, Y.-M. Kim, M.-K. Cho, J. Choi, I.-H. Jung, Corrosion of RH bottom vessel refractories – Part I: kinetic model to predict slag and metal compositions during the RH process, in: *UNITECR 2011*, Kyoto, Japan, 2011.
- [48] M.-K. Cho, T.-H. Eun, M.-A. Van Ende, I.-H. Jung, Corrosion of RH bottom vessel refractories – Part II: refractory wear by RH slags and high-alloy steels, in: *UNITECR 2011*, Kyoto, Japan, 2011.
- [49] J.R. Taylor, A.T. Dinsdale, Thermodynamic and phase diagram data for the CaO-SiO<sub>2</sub> system, *Calphad* 14 (1990) 71-88.
- [50] R. Lück, U. Gerling, B. Predel: *Z. Metallkd.* 80 (1989) 270.
- [51] K.E. Spear, T.M. Besmann, E.C. Beahm, Thermochemical modeling of glass: application to high-level nuclear waste glass, *MRS Bull. (April)* (1999) 37-44
- [52] T.M. Besmann, K.E. Spear, Thermochemical modeling of oxide glasses, *J. Amer. Ceram. Soc.* 85 (2002) 2887-2894.

- [53] E. Yazhenskikh, K. Hack, M. Muller, Critical thermodynamic evaluation of oxide systems relevant to fuel ashes and slags. Part 4: sodium oxide-potassium oxide-silica, *Calphad* 32 (2008) 506-513.
- [54] E. Yazhenskikh, Development of a new database for thermodynamic modelling of the system  $\text{Na}_2\text{O-K}_2\text{O-Al}_2\text{O}_3\text{-SiO}_2$ . Ph.D. Thesis, RWTH Aachen, Germany, 2005.
- [55] R.H. Davies, A.T. Dinsdale, J.A. Gisby, J.A.J. Robinson, S.M. Martin, MTDATA thermodynamic and phase equilibrium software from the national physical laboratory, *Calphad* 26 (2002) 229-271.
- [56] C.J.B. Fincham, F.D. Richardson, Sulfur in silicate and aluminate slags, *J. Iron Steel Inst.* 178 (1954) 4-15.
- [57] K.P. Abraham, M.W. Davies, F.D. Richardson, Sulfide capacities of silicate melts, *J. Iron Steel Inst.* 196 (1960) 309-312.
- [58] P.T. Carter, T.G. MacFarlane, *J. Iron Steel Inst.* 185 (1957) 62-66.
- [59] S.D. Brown, R.J. Roxburgh, I. Ghita, H.B. Bell, *Ironmaking Steelmaking* 9 (1982) 163-167.
- [60] M. Gonerup, O. Wijk, Sulfide capacities of  $\text{CaO-Al}_2\text{O}_3\text{-SiO}_2$  slags at 1550, 1600 and 1650, *Scand. J. Metall.* 25 (1996) 103-107.
- [61] M. Chapman, O. Ostrovski, G. Tranell, S. Jahanshahi, Sulfide capacity of titania-containing slags, *Elektrometallurgiya* 3 (2000) 34-39.
- [62] K.P. Abraham, F.D. Richardson, Sulfide capacities of silicate melts I, *J. Iron Steel Inst.* 196 (1960) 313-317.
- [63] M. Hillert, B. Jansson, B. Sundman, J. Agren, A two-sublattice model for molten solutions with different tendency of ionization, *Metall. Trans. A* 16A (1985) 261-266.
- [64] W. Huang, M. Hillert, X. Wang, Thermodynamic assessment of the  $\text{CaO-MgO-SiO}_2$  system, *Metall. Mater. Trans. A* 26A (1995) 2293\_2310.
- [65] H. Mao, M. Hillert, M. Selleby, B. Sundman, Thermodynamic assessment of the  $\text{CaO-Al}_2\text{O}_3\text{-SiO}_2$  system, *J. Amer. Ceram. Soc.* 89 (2006) 298-308.
- [66] H. Mao, O. Fabrichnaya, M. Selleby, B. Sundman, Thermodynamic assessment of the  $\text{MgO-Al}_2\text{O}_3\text{-SiO}_2$  system, *J. Mater. Res.* 20 (2005) 975-986.
- [67] M. Selleby, An assessment of the  $\text{Ca-Fe-O-Si}$  system, *Metall. Mater. Trans. B* 28B (1997) 577-596.
- [68] B. Hallstedt, Thermodynamic assessment of the  $\text{CaO-MgO-Al}_2\text{O}_3$  system, *J. Amer. Ceram. Soc.* 78 (1995) 193-198.